JGR Solid Earth

RESEARCH ARTICLE
10.1029/2019JB017737

Key Points:
- Since 2015, numerous small earthquakes have been reported in Reeves County in West Texas but their cause and year of onset was uncertain
- We analyze seismograms recorded between 2000 and 2017 to show that anomalous activity began in 2009 and has increased considerably since
- Petroleum production and related activities in the Delaware Basin probably induce this seismicity, but the exact mechanism is uncertain

Supporting Information:
- Supporting Information S1
- Data Set S1

Correspondence to:
C. Frohlich,
cliff@ig.utexas.edu

Citation:
Frohlich, C., Hayward, C., Rosenblit, J., Aiken, C., Hennings, P., Savvaidis, A., et al. (2020). Onset and cause of increased seismic activity near Pecos, West Texas, United States, from observations at the Lajitas TXAR seismic array. *Journal of Geophysical Research: Solid Earth*, *125*, e2019JB017737. https://doi.org/10.1029/2019JB017737

Received 26 MAR 2019
Accepted 10 OCT 2019
Accepted article online 4 NOV 2019
Corrected 24 FEB 2020

This article was corrected on 24 FEB 2020. See the end of the full text for details.

© 2019. The Authors.
This is an open access article under the terms of the Creative Commons Attribution License, which permits use, distribution and reproduction in any medium, provided the original work is properly cited.

Onset and Cause of Increased Seismic Activity Near Pecos, West Texas, United States, From Observations at the Lajitas TXAR Seismic Array

Cliff Frohlich[1,2], Chris Hayward[2], Julia Rosenblit[3], Chastity Aiken[4], Peter Hennings[5], Alexandros Savvaidis[5], Casee Lemons[5], Elizabeth Horne[5], Jacob I. Walter[6], and Heather R. DeShon[2]

[1]Institute for Geophysics, Jackson School of Geosciences, University of Texas at Austin, Austin, TX, USA, [2]Huffington Department of Earth Sciences, Southern Methodist University, Dallas, TX, USA, [3]Department of Geology, Portland State University, Portland, OR, USA, [4]Geosciences Marine-LAD, IFREMER, Plouzané, France, [5]Bureau of Economic Geology, Jackson School of Geosciences, University of Texas at Austin, Austin, TX, USA, [6]Oklahoma Geological Survey, University of Oklahoma, Norman, OK, USA

Abstract In recent years, numerous small earthquakes have occurred near the town of Pecos in West Texas; however, when this activity began and whether it was caused by increased petroleum industry activity has been uncertain because prior to 2017 there were few permanent seismograph stations in the region. We identify and locate earthquakes using data recorded since 2000 at TXAR, a sensitive 10-station seismic array situated about 240 km south of Pecos. We thus show that in 2007, one earthquake occurred near Pecos, in 2009 several more occurred, and subsequently, activity has increased considerably, with more than 2000 events identified in 2017. A time-of-day and year-by-year analysis identifies geographic areas in West Texas where events are likely to be natural earthquakes and quarry blasts. However, for the Pecos events, annual seismicity rates increase along with annual volumes of petroleum production and fluid waste disposal, suggesting a causal link. Analysis of seismograms collected by the EarthScope Transportable Array indicates that the 2009 earthquakes had focal depths of 4.0–5.2 km below sea level, within or just below strata where petroleum is produced and/or wastewater is injected. The largest earthquake to date had magnitude M_L3.7, but the recent high activity rates suggest that greater magnitudes may be possible. For the years 2000–2017, we provide a catalog of 10,753 epicenters of seismic events recorded at TXAR.

Plain Language Summary Petroleum production in the Permian Basin of West Texas has been accelerating since 2007, and by 2023 it is anticipated that Permian Basin production will exceed the production of every nation in the world other than Saudi Arabia. Developing this domestic source of energy has profound economic and political implications, especially since protecting vital foreign sources of energy has been a major factor affecting U.S. foreign policy. In recent years, numerous small earthquakes have occurred in the Delaware Basin (a subregion of the Permian Basin), but when this seismicity began has been uncertain because there were few seismographs in this region before 2017. We show that these anomalous earthquakes first occurred in 2009 and that many of them are probably induced by petroleum production in the Delaware Basin. Understanding the relationship between production and earthquake activity is a critical first step toward mitigating seismic hazards that could affect local populations and compromise the development of these vital petroleum resources.

1. Introduction

Since 2008, there has been a significant increase in the number of earthquakes reported in the central United States (Ellsworth, 2013). This increase is generally attributed to wastewater disposal or enhanced oil recovery operations that produce changes to subsurface pressure and reduce friction that inhibits slip along existing faults. In some locations like east Texas and the Fort Worth Basin in north Texas (Frohlich, 2012; Frohlich et al., 2014; Hornbach et al., 2015; Scales et al., 2017), these induced earthquakes were clustered within a few kilometers of individual high-volume wells, suggesting that injected fluids caused pressure changes that diffuse away from wells and reach suitably oriented stressed faults. Elsewhere, as in Oklahoma and Kansas, seismic activity is distributed over a broad area, apparently because the very high

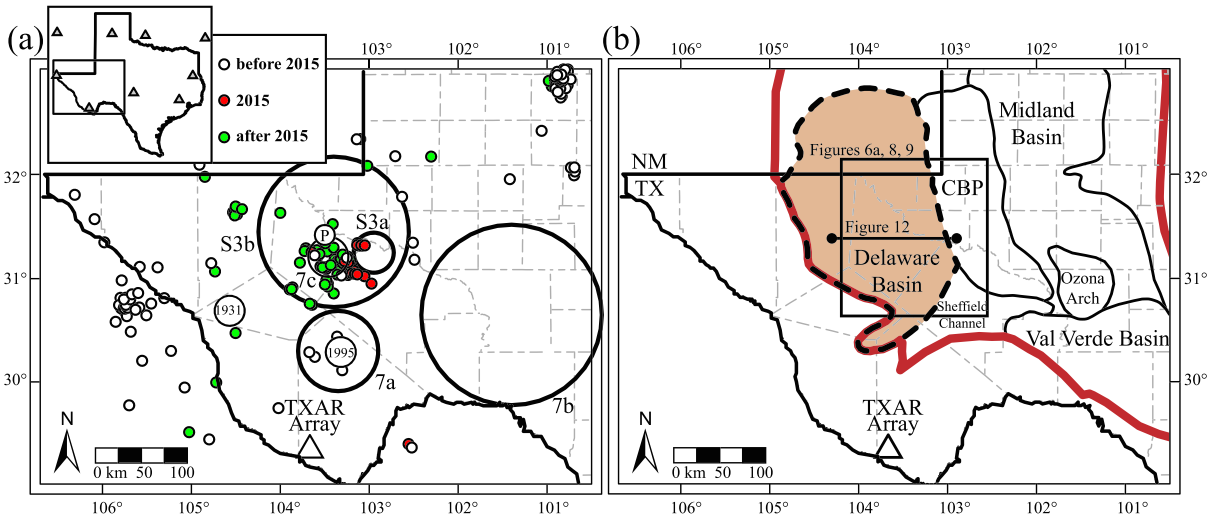

Figure 1. West Texas seismicity and petroleum production. (a) Map of earthquake epicenters (small circles) reported by the U.S. Geological Survey. Circles labeled "1931" and "1995" indicate locations of the ~M6 1931 and 1995 earthquakes. Triangle is location of Lajitas TXAR seismic array. Circle labeled "P" is town of Pecos, TX. Larger circles labeled 7a, 7b, 7c, S3a, and S3b are subregions where temporal properties of seismicity are evaluated (see Figures 7a, 7b, 7c, S3a and S3b). Dashed lines in this and subsequent maps are county borders. Inset shows the geographic location of this map; grey triangles on inset are locations of broadband seismograph station operating in 2005. (b) Map of the Permian Basin of West Texas. The thick red line delineates the Permian Basin; its major subregions are: the Delaware Basin (shaded area), the Central Basin Platform (CBP), the Midland Basin, and Val Verde Basin. Rectangle indicates areas mapped in Figures 6a, 8 and 9; labeled line shows location of cross section Figure 12.

volumes of injected fluids have elevated pressures above the threshold required for fault activation within entire formations or because poroelastic stresses trigger earthquakes at distances of tens of kilometers (Walsh & Zoback, 2016; Goebel et al., 2017; Peterie et al., 2018; Rubinstein et al., 2018). Induced earthquakes have also been associated with the extraction of oil and gas and with hydraulic fracturing operations (Frohlich et al., 2016; Skoumal et al., 2018).

In 2015, the U.S. Geological Survey (USGS) reported a cluster of 12 earthquakes having magnitudes m_{bLg} 2.5–3.3 in the Delaware Basin of West Texas south of the town of Pecos, a location where few earthquakes had been reported previously (Figure 1a). Subsequently, there has been a steady increase in the number of earthquakes in this Pecos Cluster (i.e., within Circle S3b in Figure 1a), with the USGS reporting 36 and 44 earthquakes with $m_{bLg} \geq 2.5$ in 2017 and 2018, respectively.

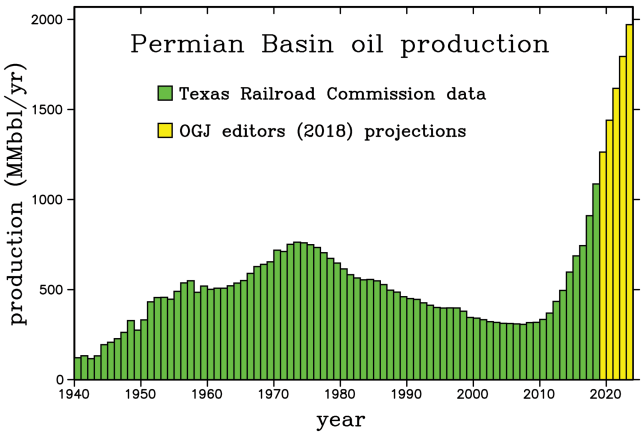

Figure 2. Annual Permian Basin crude oil production 1940–2023. Data include production from both Texas and New Mexico. The increase beginning in 2009 is associated with extraction of oil and gas from unconventional wells (e.g., Scanlon et al., 2017).

Considerable volumes of oil and gas have been produced from the Permian Basin over the past 100 years, though consistent records are only available from the 1940s onward (Figures 1b and 2). Since 2010, petroleum production has been increasing and this is expected to continue—oil and gas production volumes are projected to double between 2018 and 2023, exceeding volumes in any other U.S. location and reaching levels that exceed the production of any Organization of Petroleum Exporting Country other than Saudi Arabia (OGJ editors, 2018). Thus, for both scientific and economic reasons it is important to evaluate seismic hazard in the Permian Basin and understand the relationship—if any—between petroleum production and seismicity. There are also water issues associated with the recent production increase (see review in Scanlon et al., 2017). Much of this production is now unconventional and involves hydraulic fracturing that requires large volumes of water, and water coproduced from Pecos area oil and gas wells is permanently disposed into the subsurface via saltwater disposal wells, inducing pore pressure changes within the target reservoirs. Water used for hydraulic fracturing in West Texas is obtained from local aquifers or is recycled produced water.

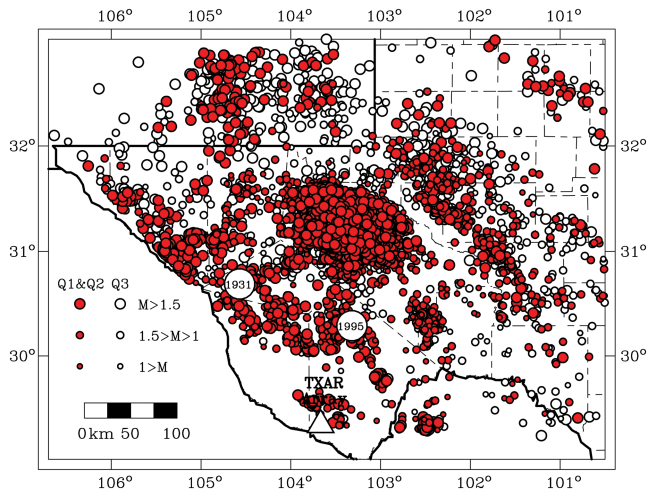

Figure 3. Map of epicenters (2000–2017) determined in this study from the analysis of TXAR data. Symbol size and color indicates magnitude M_{TXAR} and quality Q1 (better) to Q3 (worse) assigned by analyst to P and S time picks (see section 2.2).

Altogether, wastewater disposal is a significant activity because volumes of produced water are many times greater than volumes of produced oil or gas (Scanlon et al., 2017).

The cause of the Pecos Cluster earthquakes has been uncertain because both natural and induced earthquakes occur in West Texas. Among the natural events are the two largest earthquakes in the state (Figure 1a): the 16 August 1931 Valentine earthquake with moment magnitude M_W6.3 (Doser, 1987) and the M_W5.7 14 April 1995 Alpine earthquake (Frohlich & Davis, 2002). However, analysis of data collected from 1976 to 1979 by a 12-station regional network indicated that many small earthquakes occurring in the Central Basin Platform and Delaware Basin (Figure 1b) were related to enhanced recovery or petroleum production operations (Doser et al., 1992; Frohlich et al., 2016; Keller et al., 1987).

Because regional seismograph station coverage was sparse prior to the installation of the statewide TexNet seismic network in 2017 (Frohlich et al., 2016; Savvaidis et al., 2019; see also inset Figure 1a), it has been unclear when the Pecos Cluster activity commenced and how it has developed (e.g., Lund-Snee & Zoback, 2016, 2018). We resolve this uncertainty by analyzing seismic records from 2000 to 2017 at the Lajitas TXAR seismic array, a facility 240 km south of Pecos comprised of 10 very high gain seismic stations (Tibuleac & Herrin, 1997). Analysis of TXAR data has allowed us to produce a catalog of seismic events (Figure 3 and Table S1) that is far more complete than the USGS catalog. The TXAR catalog includes more than 7,000 seismic events in the Pecos Cluster. We show that multiple earthquakes first occurred in this region in 2009, when 19 earthquakes with magnitude $M \geq 1.0$ were recorded, and we demonstrate that the activity rate has subsequently increased, with more than 1,600 earthquakes having $M \geq 1.0$ recorded in 2017. We also show that this cluster has spatially expanded since 2011, coinciding with increasing rates of high-volume petroleum production and wastewater disposal over a broader region.

2. Data and Methods

2.1. Seismic Data

This investigation determined epicenters for seismic events using three different sources of data: (1) seismograms recorded April 2000–2017 by the TXAR seismic array near Lajitas, TX (Tibuleac & Herrin, 1997); (2) seismograms recorded March 2008 – March 2010 by the EarthScope Transportable Array (TA) network; and (3) seismograms recorded September 2017 to December 2018 by the TexNet, the Texas statewide seismic network (Savvaidis et al., 2019).

Prior to 2017 earthquakes having magnitudes less than 2.5 were seldom located by the USGS, and the epicentral inaccuracies of locations were often ~20 km or more (Frohlich et al., 2016; Walter et al., 2018). Except during 2008–2010, when the EarthScope TA was in West Texas, the closest seismograph stations reporting to the USGS were usually at distances of 2°–5° from the Pecos Cluster. One of these stations was LTX, colocated with station TX31 of the 10-station TXAR array (Figures 1a and 4a).

We use TXAR array data (Figure 4b) to compile the TXAR catalog (Figure 3 and Data Set S1) of epicenters for seismic activity in West Texas for the April 2000 to December 2017 time period. Locations of selected 2009 earthquakes determined using EarthScope data provide critical information about the initiation of seismic activity for the Pecos Cluster. Epicenters determined using the 2017 TexNet data (Savvaidis et al., 2019) provide ground truth information to assess the accuracy and completeness of the TXAR catalog.

2.2. Determining Epicenters Using Lajitas TXAR Array Data

Due to unusually favorable geological conditions and its remote location with low ambient noise, the TXAR array is extraordinarily sensitive (Tibuleac et al., 1997). For the time period considered, TXAR consists of 10 short-period vertical and one broadband three-component continuously recording seismic station (TX31) deployed in shallow 6-m-depth boreholes within a region having dimensions of about 4 × 6 km (see Figures 1a and 4a). We determined epicenters by evaluating the passage of the *P* wave across the 10-

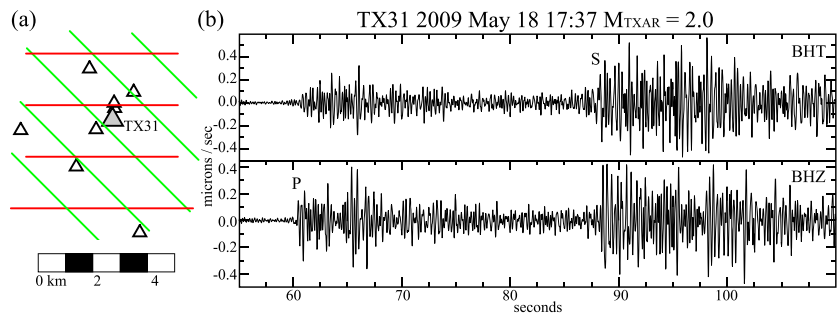

Figure 4. Earthquake location with the Lajitas TXAR array. (a) Map view of the seismic stations in the TXAR array. Note that two high-gain stations (white triangles) are hidden by the broadband station (grey triangle) at this scale. Red and green lines depict *P* wave fronts crossing the array from earthquakes occurring to the north and northeast, respectively. Automated detection of relative arrival times across TXAR array stations constrains the source-to-station direction for the event. (b) Transverse- (BHT) and vertical-component (BHZ) seismograms for a Pecos Cluster earthquake at station TX31 of TXAR. Analyst-refined picks for *P* and *S* arrivals and the (*S*-*P*) interval at TX31 constrain the source-to-station distance for the event.

station array to constrain the station-to-source direction (back azimuth) and using the (*S*-*P*) interval picked on TX31 to fix the source-to-station distance (Figure 4). This TXAR-only location method does not allow us to determine accurate focal depths; the TXAR catalog thus includes epicenters only.

To identify candidate events, we applied a multistage F-K filtering process. We first applied a bandpass filter with corners at 2 and 10 Hz to the 40 sample/s data stream and downsampled the result with an antialias filter at 7.5 Hz to 15 samples/s. The downsampling substantially reduced both memory and CPU resources needed to process the data. The F-K spectra were calculated in a moving 8.5 s (128 sample) window updated every 2.5 s. To detect candidate events, we applied three different detector algorithms based upon the F-K spectra (see details in the supporting information). Candidate events were signals that met the detection thresholds for any one of the three detector algorithms.

For each candidate event we reprocessed the data to determine trial values for *P* and *S* arrival times, *P* and *S* phase back azimuths, *P* and *S* phase slownesses, maximum and root-mean-square (rms) *P* and *S* amplitudes, and other parameters used to assess data quality. Because this study focused on regional earthquakes in Texas, we only considered candidate detections associated with trial back azimuths between 315°–360° and 0°–90°, and with trial *S*-*P* intervals between 10-55 s, corresponding to sources in Texas and New Mexico between about 75 and 450 km from the TXAR array.

An analyst reviewed the remaining candidate events and picked *P* and *S* times on broadband station TX31, assigning quality factors of Q1 (better) to Q3 (worse). The analyst discarded detections that did not appear to be seismic events, detections for which broadband data were unavailable, or detections where either the *P* or *S* could not be identified with confidence. The analyst also discarded events where the *P* arrival differed by more than 2 s from the machine-picked *P* time used to determine the back azimuth estimate.

For the entire 2000–2017 interval and for events having $M_{TXAR} > 0.8$, the analyst identified *P* and *S* for a fraction of all computer-detected events, but this fraction varied over time and depended on event location (Figure S1 and Table S1). Between 2000 and 2010 the average annual value for this fraction was 0.38 and then increased to 0.73 for 2011–2017. We speculate this change occurred because *P* and *S* identification differed for earthquakes and for quarry blasts (which occur mostly in the daytime and were more common after 2010) and also differed for Pecos Cluster earthquakes and earthquakes situated elsewhere. In support of this speculation, we note that for events occurring 01:00–13:00 UTC (during the night, local time 7 p.m. to 7 a.m.) with locations outside of Pecos Cluster Circle S3b, the average annual fraction for 2000–2017 was 0.46 ± 0.10 (Figure S1), and there was no obvious increase beginning in 2011. In contrast, for 2011–2017 nighttime-only events within Pecos Cluster Circle S3b, the fraction was 0.88 ± 0.03.

To develop relationships for determining epicenters from the back azimuth and (*S*-*P*) estimates, we evaluated a subset of 140 Pecos Cluster earthquakes that were located by the statewide TexNet seismic network

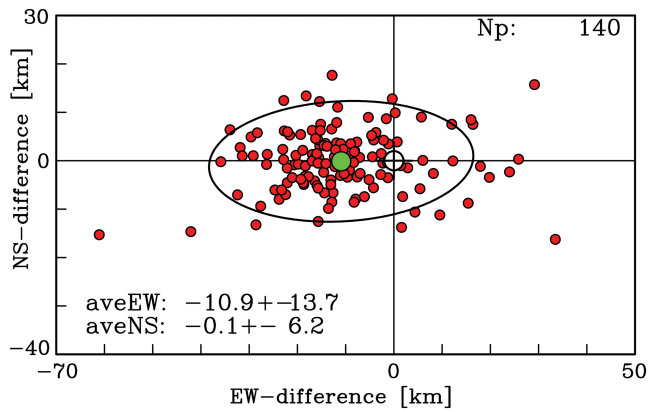

Figure 5. Comparison of epicenters determined using (*S*-*P*) intervals and apparent direction at TXAR with epicenters determined by the TexNet seismic network using conventional location methods. Data are for 140 earthquakes within Pecos Cluster Circle S3b; all plotted events had *P* and *S* picks that the analyst assigned quality 1 or 2 (red circles in Figure 3). The ellipsoid indicates the 2σ fit for these data; the green dot at −10.9 km is the center of the ellipsoid—this indicates that before back azimuths for TXAR locations are adjusted by adding 3° (see text), they average 10.9 km west of TexNet locations.

and also were in the TXAR catalog and which occurred between September and December 2017, when the majority of regional stations in the TexNet seismic network had been deployed (Savvaidis et al., 2019). For all these earthquakes, an analyst repicked *P* and *S* and then relocated the events using the double-difference method (Waldhauser & Ellsworth, 2000) and the velocity model currently used for routine location in the Delaware Basin by the TexNet program (see Table S2 in Savvaidis et al., 2019). For these 140 epicenters located by TexNet and also detected by TXAR (Figure 5), the best fitting relationship determined by linear regression between epicenter-to-TXAR distance Δ (in km) and (*S*-*P*) interval (in seconds) was

$$\Delta = 8.62S{-}P{-}13.4. \tag{1}$$

Comparison of these selected TexNet and TXAR locations revealed that the TXAR locations averaged 10.9 km west of the TexNet locations (Figure 5). For events 210 km from TXAR, such as the Pecos Cluster, this corresponds to a back azimuth discrepancy of 3°. Therefore, before determining the epicenters listed in the TXAR catalog (Data Set S1), we adjusted the TXAR-determined back azimuths by adding 3°. This relationship removes the azimuth bias for events in the Pecos Cluster and thus may not be correct for events elsewhere in West Texas. However, the correction is nearly identical to the back azimuth correction factor developed for TXAR by Tibuleac and Herrin (1997) for sources situated due north of the array. The ellipsoid fitting the location differences for the 140 epicenters (see Figure 5) suggests the 2σ location accuracy for TXAR catalog is about ±27.4 km EW and ±12.4 km NS. This is approximately comparable to the location accuracy for small West Texas earthquakes reported by the USGS prior to the installation of TexNet (Frohlich et al., 2016).

We also developed a relationship to estimate an event magnitude M_{TXAR} using distance Δ in kilometers and the measured rms amplitude S_{RMS} of the *S* phase, measured in nm/s on the 2–10 Hz filtered vertical short-period traces. This relationship was adjusted so that M_{TXAR} corresponded to values of m_{bLg} reported by the USGS for West Texas earthquakes. We identified 59 events in the TXAR catalog occurring between 2000 and 2017 with locations reported by the USGS (Figure S2). The best fitting relationship, as determined by linear regression, was

$$M_{TXAR} = log_{10}S_{RMS} + 1.48log_{10}\Delta{-}3.29. \tag{2}$$

2.3. Hypocenters Determined Using EarthScope Transportable Array Data

The EarthScope program deployed the TA, consisting of three-component broadband seismic stations operating for 2-year intervals situated on a 70-km grid that stretched across the continental United States. In West Texas, all nine of the stations in Figure 6a were fully operational between 22 April 2008 and 12 February 2010. During this interval we identified four earthquakes in the Pecos Cluster that were especially well recorded, with visually distinct *P* and *S* arrival times at station 327A at a distance of ~10 km, as well as visually distinct phases at all nine TA stations within 115 km of the epicenter (Figure 6). These four earthquakes were 18 May 2009 17:37 M_{TXAR} 2.01 (Figures 4b and 6b), 8 June 2009 19:32 M_{TXAR} 1.87, 1 July 2009 15:09 M_{TXAR} 2.29, and 3 July 2009 16:20 M_{TXAR} 2.13. For a fifth earthquake (18 September 2009 10:12 M_{TXAR} 2.50) we could pick *P* at all nine TA stations and *S* at all except 227A.

For these five earthquakes, we determined hypocenters using *P* and *S* from the nine EarthScope TA stations and the 1-D velocity model currently used for routine location in the Delaware Basin by the TexNet program (see Table S2 in Savvaidis et al., 2019). Because eight of the stations were at similar distances (55–110 km) and distributed nearly uniformly around the epicenter, the epicenters were minimally influenced by the choice of the velocity model used for location. As discussed further in section 3.2, the focal depths depend critically on (*S*-*P*) intervals at the closest station 327A.

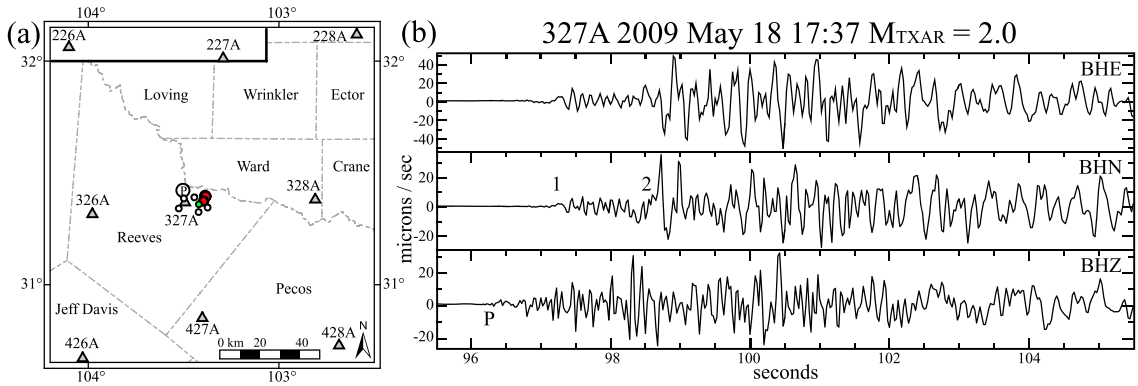

Figure 6. Pecos Cluster earthquakes with excellent records at TXAR and TA stations. (a) Map shows temporary TA stations (triangles) operating in 2009. Five earthquakes with identifiable P and S phases at these TA stations occur in the TXAR catalog. Red circles: locations determined using the nine TA stations; white circles: TXAR catalog. The green circle is the TXAR-catalog location for the 27 September 2007 earthquake. The circle labeled "P" is the town of Pecos; note that the town of Pecos is in Reeves County, whereas Pecos County is some 50 km to the southwest. (b) Broadband three-component seismograms at station 327A for earthquake of 18 May 2009 at 17:37, the first 2009 Pecos Cluster earthquake detected by TXAR. It is straightforward to pick the *P* phase on the vertical (BHZ) component; shear phases labeled "1" and "2" are clearly visible on the north (BHN) component. If phase 1 is *S*; this implies focal depth is ~4.8–6.0 km beneath the surface (4.0–5.2 km below sea level); if phase 2 is *S*, the focal depth is ~8.1–9.7 km beneath the surface.

2.4. Data Concerning Injection and Production of Fluids

The Texas Railroad Commission (RRC) archives information about both production and injection wells operated in support of petroleum production in Texas. This information includes well locations, depths, permitting history, and monthly rates of injection/production of fluids and gases. The RRC database is publicly available online and is mostly complete for the past two decades. In addition, data for treatment fluids used for hydraulic fracturing are available from FracFocus; current regulations do not require reporting these data and they are incomplete, especially prior to about 2014, but when the data are available they do provide information about hydraulic fracturing activity.

For this investigation, we compiled RRC and FracFocus data for wells in West Texas counties, removing some obvious data blunders (e.g., keypunching/transcription errors where individual monthly values were apparently entered as 10 times greater than all other monthly values in a particular year). For each well in our study area, we determined values for the years 2000–2017 for (1) production volumes for oil, (2) production volumes for gas, (3) production volumes for water, (4) injection volumes for salt water (waste) disposal, (5) injection volumes for secondary recovery, and (6) injection volumes of treatment fluids.

3. Results

3.1. Epicenters 2000–2017 Determined Using Data From the Lajitas TXAR Seismic Array

Evaluation of certain event groups within the TXAR catalog suggests that the detection capability of TXAR does not change significantly over time. For example, for the 244 TXAR catalog events within Circle 7a (see Figure 1a) surrounding the 1995 Alpine M6 earthquake, a time-of-day versus year-of-occurrence plot (Figure 7a) shows that events occur approximately uniformly throughout the day, while the rate of occurrence decreases only slowly between 2000 and 2017. This decrease likely represents a slow cessation of aftershock activity following the 1995 earthquake, roughly consistent with an Omori $1/t$ decay rate (e.g., the 13–18 events/year rate observed in 2005–2006, 10 years after the mainshock, is about twice the 7–9 events/year observed in 2015–2016 after 20 years).

A similar analysis indicates that in a few locations, the TXAR catalog includes a significant number of quarry blasts. For 284 events within Circle 7b (see Figure 1a), the majority occur between 1500 and 2300 UTC, or 9 a.m. to 5 p.m. CST (local time), and the annual numbers of events increase in 2013 and subsequently (Figure 7b). These time-of-day and year-of-occurrence variabilities are consistent with quarrying activity. Our analysis as in these figures suggests that quarries differ in the patterns they exhibit. The work in some quarries is fairly uniform over time (but in the daytime); in other quarries the work is highly concentrated in certain times (but in the daytime). These differences are reasonable; the need for road-building material or

sand for fracking will be very high when frac pads are being built and hydrofracturing is underway, and negligible at other times. But quarries providing building stone, or quarries distant from hydrofracturing operations, might have more regular patterns over time. Another probable quarry that appears to be active from 2010 to 2014 occurs within circle S3a (see Figures 1a and S3a).

The majority of cataloged events occur within Circle S3b (see Figures 1a and S3b) centered near Pecos with a radius of 75 km; 8,002 of the 10,753 events in the TXAR catalog are in this Pecos Cluster. The seismicity within the Pecos Cluster Circle S3b is not spatially uniform, as nearly half of the events (3,641) occur within a 20-km radius subregion labeled Circle 7c (Figures 1a and 7c). Within Circle 7c, there are few events prior to 2009, event rates increase in time, events are distributed uniformly through the day, and there are no apparent large earthquakes followed by traditional aftershock sequences.

Comparison of the TXAR and TexNet catalogs for 2017 demonstrates that TXAR event detection capability is significantly more sensitive than the TexNet network, although TXAR does miss some events reported by TexNet. For epicenters in Circle 7c (see Figure 1a) occurring September–December 2017 during nighttime hours (00–13 UTC), TXAR detected 307 events, of which 188 (61%) were in the TexNet catalog. In comparison, TexNet detected 160 nighttime events in Circle 7c over this same time period, of which 134 (84%) were in the TXAR catalog. We presume that the 16% missed rate for TXAR is attributable to various kinds of noise and interfering events that affect the single-array F-K event detection/identification algorithm. Individuals using the TXAR catalog (Data Set S1) should be aware that it misses some earthquakes, even some with magnitudes of 1.5 and greater, but it contains considerably more seismic events than other available regional catalogs. Both the TexNet and TXAR catalogs report to lower magnitudes and exhibit lower completeness magnitudes than the USGS catalog. During the same time period in late 2017, the USGS catalog reported nine nighttime earthquakes, all greater than magnitude 2, with epicenters in Circle 7c, for example.

3.2. The Initiation of Seismicity in the Pecos Cluster

The time-of-day and year-of-occurrence pattern for Circle 7c (Figure 7c) suggests that the Pecos Cluster activity commences in 2009 or 2010 and indicates these events are mostly earthquakes (not quarry blasts). Annual occurrence rates are 2 earthquakes/year or less from 2000–2008, 7/year in 2009, and 38/year in 2010. Subsequently, the annual rates all exceed 200/year, and there are more than 1,400 events in 2017. The activity occurs randomly throughout the day, as expected for earthquakes. The larger Circle S3b (Figure S3b) includes a quarry within smaller Circle S3a; the rose diagram in Figure S3a is dominated by seismic events occurring during the afternoon, local time. Nevertheless, the overall patterns for Circles S3b and 7c are similar; in Circle S3b, rates are 2–20 earthquakes/year between 2000 and 2008, 27/year in 2009, 129/year in 2010, and then exceed 400/year every year after 2011, reaching more than 3,000/year in 2017. The gradual rate increase over several years is unlike a typical aftershock sequence, where the highest rates occur immediately after a large event, and then rates decline regularly over time.

Inspection of the TXAR catalog (see Figures 8 and S4) confirms that several earthquakes occurred near the town of Pecos in 2009; in subsequent years events occurred at higher rates, and locations migrated to fill a larger area to the south. If we exclude the suspected quarry within Circle S3, activity is mostly confined in Reeves County south of the town of Pecos until about 2013 (Figure S4). Only after 2013 are there are numerous epicenters to the southeast within Pecos County and new areas of activity to the north and west of the city of Pecos within Reeves County.

The five earthquakes occurring in 2009 recorded by EarthScope TA stations allow us to further refine the time and location for the onset of the Pecos Cluster. The epicenters for all five earthquakes occur near 31.395°N, 103.390°W (red circles in Figure 6a). For these earthquakes, the seismograms at the closest station (TA 327A at ~10 km) were all highly similar in appearance (see Figure 6b), consistent with their having sources originating from nearly identical locations.

The focal depths for the five earthquakes, however, depend critically on (*S*-*P*) intervals at station 327A; there is some ambiguity concerning the picks for *S*. On 327A seismograms, particle-motion plots show there are two phases with transverse particle motions (labeled "1" and "2" in Figure 6b) that might be picked as *S*. If phase 1 is *S*, the focal depths for four of the events occur between 4.8 and 6.0 km relative to the surface (4.0–5.2 km below sea level—BSL); if phase 2 is *S*, the focal depths are between 8.1 and 9.7 km relative to the surface (7.3–8.9 km BSL). We favor phase 1 as it is the first arriving, more direct *S* arrival, traveling

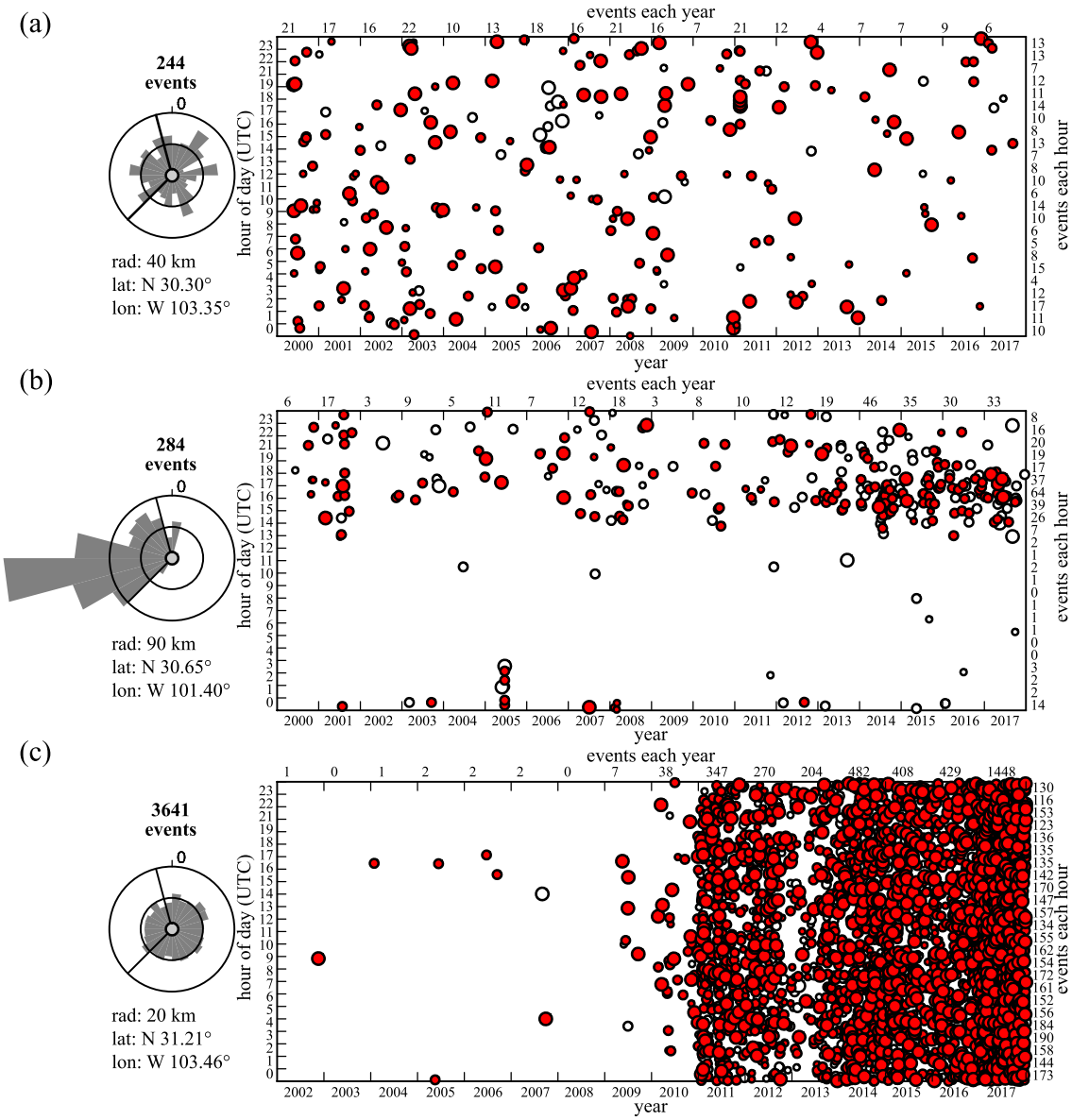

Figure 7. Time-of-day versus year-of-occurrence for selected seismic events. The three panels describe temporal properties of seismic events within Circles 7a, 7b, and 7c in Figure 1a. Rose diagrams on the left plot event numbers within 24 one-hour intervals; tic labeled "0" above circle is 0000 UTC, the two straight radial lines are at 9 a.m. and 5 p.m. CST (local time). The circle with half the diameter of the largest circle indicates a uniform level where equal numbers of events occur in all hours. Labels indicate total number of TXAR catalog events within each circle as well as circle radius and center coordinates. Rectangle plots on the right show time-of-day (vertical axis) versus year-of-occurrence for individual events (circles); event numbers within each hour and year are listed at right and above rectangles, respectively. Symbol sizes and colors indicate event magnitude and quality as in Figure 3. (a) Events within the 40-km-radius circle surrounding 1995 April 14 M6 Alpine earthquake (Circle 7a in Figure 1a). Because these events occur approximately randomly with respect to time of day, with rates slowly decreasing from year to year, we conclude that TXAR event detection is nearly uniform over time, and these events are aftershocks of the 1995 earthquakes. (b) Events within the 90-km-radius Circle 7b in Figure 1a. Because almost all events occur between 9 a.m. and 5 p.m. local time, these appear to be caused by human activities such as quarry blasting. Note that activity rates increase beginning about 2013. (c) Events within a 20-km-radius Circle 7c in Figure 1a, the most active region of the Pecos Cluster. It is likely these are earthquakes because they are distributed uniformly over the day.

the shorter path from source to station. The depths determined using phase 1 (4.0–5.2 km BSL) are supported by independent data from the TexNet catalog. In 2018 TexNet located six earthquakes with $M_L \geq 1.2$ within 3 km of the 2009 earthquakes and all reported focal depths between 3.3 and 6.1 km BSL.

To assess whether these 2009 earthquakes were the first events in this location, we cross correlated the three-component TX31 seismograms for these five earthquakes with seismograms for all prior events in the TXAR

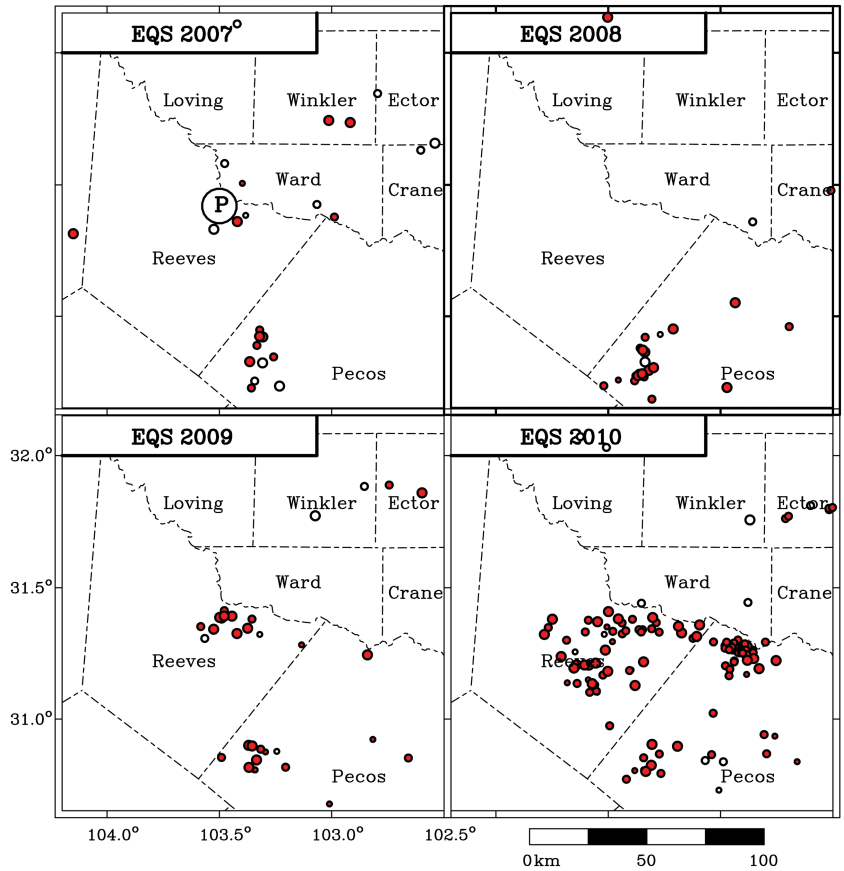

Figure 8. Maps of TXAR-determined epicenters near Pecos, 2007–2010. Small circles are seismic events; sizes and colors are as in Figure 3. The large circle labeled "P" on 2007 map is the town of Pecos, TX. Note also that near the town of Pecos, multiple earthquakes occur in 2009, and activity grows in number and aerial extent in 2010. See Figure S4 for maps of all years 2000 through 2017.

catalog. The only significantly high correlation was 0.71 between records for the 2009 May 18 earthquake (Figures 4b and 6b) and an event occurring 2007 September 27 at 05:59 UTC with M_{TXAR} of 2.30. This waveform similarity suggests that the 2009 activity originated from nearly the same location as the 2007 earthquake.

3.3. Relationship of Seismicity to Oil and Gas Industry Activity

Maps of oil production, gas production, saltwater disposal volumes, and hydraulic fracturing fluid volumes (see Figures 9, 10, 11, S5, S6, S7, and S8) provide no obvious explanation as to why Pecos Cluster activity commenced in Reeves County, either in September 2007 or May 2009. When the seismicity began, petroleum production and injection had been ongoing for years along the county line between Reeves and Ward Counties.

RRC monthly data on oil and gas production, and salt water disposal (SWD) and FracFocus data do not differentiate between conventional and unconventional production or source of disposed fluids. Within 10 km of the 2009 epicenters, RRC data indicate that more than 25,000 bbl of oil and 100,000 mcf of gas were produced for every month, back to before 2000. Wastewater disposal rates exceeded 150,000 bbl every month from 2000 to 2005, 185,000 bbl/mo between 2006 and November 2008, and 400,000 bbl/mo after December 2008. None of these rates changed abruptly prior to May 2009 in the Pecos area (Figure 10). The FracFocus data show that on the order of 10 hydrofracturing wells were initiated each month within 10 km of the 2009 epicenters in 2009 and 2010 (see Figure 10). Thus, it is possible that hydraulic fracturing, or the disposal of waste fluids resulting from hydraulic fracturing, induced the May 2009 earthquakes. In June and August of 2009, two SWD wells situated 6 and 5 km north of the epicenters became active

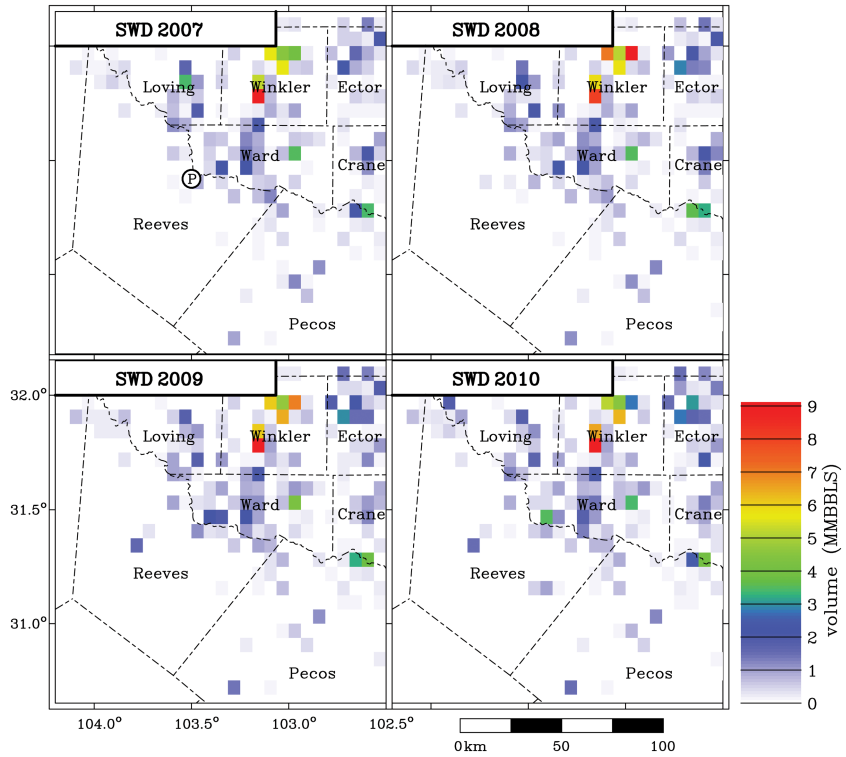

Figure 9. Maps of annual injected wastewater disposal volumes (SWD) near Pecos, 2007–2010. Volumes are determined for 1/16° squares; warmer colors are higher volumes as indicated in bar at right. Note wastewater fluids are injected near where seismic activity begins in 2009, especially to the north in Ward County, but volumes are not particularly high or different than in previous or subsequent years. Figures S5–S8 present maps for all years 2000–2017 for injected wastewater, produced oil, produced gas, and hydraulic fracturing treatment fluid volumes.

(API#42-475-34339 and API#42-475-30517); for several years these wells each subsequently disposed of volumes ranging between 33,000 and 256,000 bbl/mo. This disposal activity serves as an example of the SWD development and volumes associated with growth of unconventional plays in the Delaware Basin (Figure 9).

Between 2011 and 2017, petroleum production and fluid injection, from both waste disposal and hydraulic stimulation, increased considerably in Reeves County, and this coincided spatially and temporally with increasing seismicity rates (Figure S4). For example, within Circle 7c oil production exceeded 1 million bbls/mo for all but 6 months after August 2012, and wastewater disposal volumes exceeded 1 million barrels/mo after December 2012 (see Figure 11).

The increasing rates of seismic activity in the Pecos Cluster were interrupted by two notable periods of decreasing activity, the first occurring early in 2013, and the second in the last half of 2015 and first half of 2016 (Figures 7c, 11, and S3b). Both time periods coincide roughly with decreases in wastewater disposal volumes following decreases in hydraulic fracture fluid volumes (Figure 11). In 2017, there was a considerable increase in seismic activity; within Circle 7c, there were 429 events in 2016 and 1,448 events in 2017. This increase was accompanied by 2017 increases in produced oil and gas, and injection of wastewater and hydraulic fracturing treatment fluids.

4. Discussion

4.1. Time History of Pecos Cluster Seismicity

The principal result of this investigation is to describe the initiation and growth-in-area history of an earthquake cluster near the town of Pecos in the Delaware Basin of West Texas. The resulting TXAR catalog (Data Set S1) is considerably more complete than previously available catalogs for earthquakes occurring during

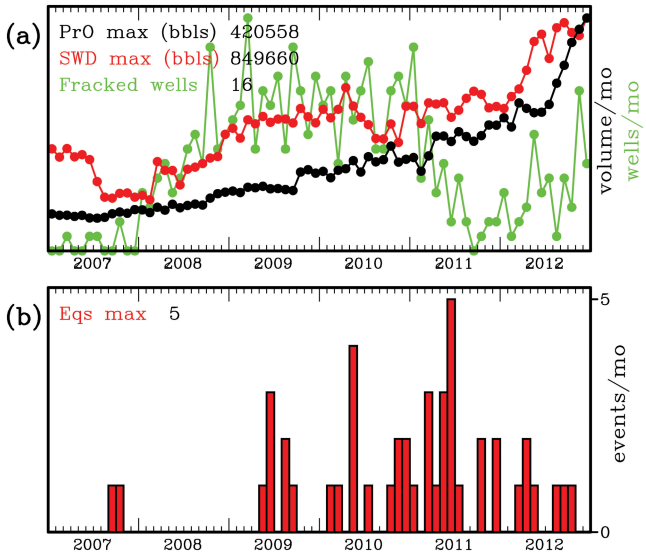

Figure 10. Petroleum production activity near the 2009 epicenters (within 10 km of 31.395 N, 103.390 W). (a) Monthly volumes for produced oil (PrO), wastewater disposal (SWD), and the number of hydraulically fractured wells initiated. Plotted values are normalized to maximum monthly values, given at upper left. (b) Monthly earthquake numbers in TXAR catalog.

2000–2017 in West Texas. We show multiple earthquakes first occurred in the Pecos Cluster in 2009, although there was a single very similar earthquake in the same location in 2007 (Figures 6a, 8 and S4). Since 2009, activity rates have increased considerably as the cluster has expanded geographically to occupy an area with a diameter of roughly 100 km (Figures 3 and S4).

A second important result of this investigation is to provide more accurate locations for the earliest occurring earthquakes in the Pecos Cluster (Figures 6 and 12). The five events recorded in 2009 by the EarthScope TA occurred near 31.395°N, 103.390°W, about 10 km east of the town of Pecos, with focal depths of 4.0–5.2 km BSL. If these depths are accurate, they indicate that the Pecos Cluster activity initiated between the top of the crystalline basement, at about 5.5-km depth BSL, to just beneath the Permian-age Wolfcamp Group (Figure 12), one of the significant oil and gas stacked shale intervals being produced using hydrofracturing. This sedimentary interval includes the Woodford Formation and Ordovician-age Ellenberger Group, which were a common conventional hydrocarbon target. The Ellenberger Group is now sometimes used for wastewater disposal, particular in the northern part of the Delaware Basin, but the large majority of SWD activity within our study area occurs in the shallower Permian-age Delaware Mountain Group (see Scanlon et al., 2017, for further discussion).

4.2. Relationship With Petroleum Production and Fluid Injection Activity

Our investigation documents similarly increasing rates in petroleum production activity and seismic activity in the Pecos Cluster (Figures 11 and S4–S8), but there are important aspects of this relationship that remain uncertain. In Ward County, just north where the cluster began near the town of Pecos, significant amounts of petroleum production, hydraulic fracturing, and wastewater disposal had been ongoing long before 2000. Lateral well technologies enabled new production from the unconventional Wolfcamp and Bone Spring stratigraphic intervals southwest of Ward County, in the central portion of the Delaware Basin. Since lateral well [illegible] 2009, production and injection volumes have been rapidly increasing in the Delaware Basin generally, coinciding spatially and temporally in Reeves County with the considerable increase in seismicity rates after about 2011 (Figures 9, 11, and S4–S8). But we are unable to identify any single petroleum-related activity (e.g., wastewater disposal or petroleum production) that is principally responsible for the initiation and growth of the cluster that began near Pecos in 2009.

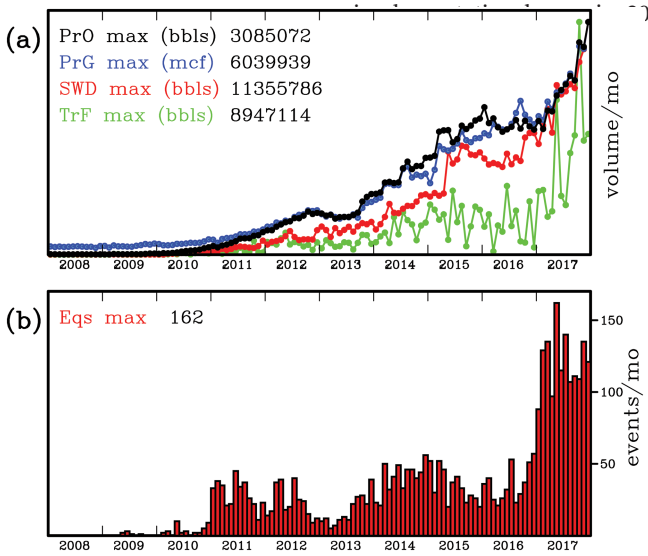

Figure 11. Petroleum-production operations and seismicity in Circle 7c. (a) Monthly volumes for produced oil (PrO), produced gas (PrG), wastewater disposal (SWD), and hydraulic fracturing treatment fluid (TrF). Plotted values on vertical axes are normalized to maximum monthly values, given at upper left. (b) Monthly earthquake numbers in TXAR catalog.

It is notable that outside of the Pecos Cluster, levels of seismic activity are considerably lower to the north in Ward, Loving, and Winkler Counties, even though considerable petroleum is produced there and has been produced for decades. There have been occasional reports of small possibly induced earthquakes in the Central Basin Platform and near the Ward-Winkler county boundary within the Delaware Basin (e.g., Doser et al., 1992), but no previous examples having the aerial extent or seismicity rates observed in the Pecos Cluster. Lund-Snee and Zoback (2018) present observations indicating that the orientation of the maximum horizontal stress S_{Hmax} is NW-SE where the Pecos Cluster occurs in Reeves County but rotates to more toward E-W in northern Reeves and in Loving and Winkler Counties. This may broadly explain why the behavior in the Pecos Cluster across central and southern Reeves County and northwestern Pecos County differs from the northern portions of the Delaware Basin.

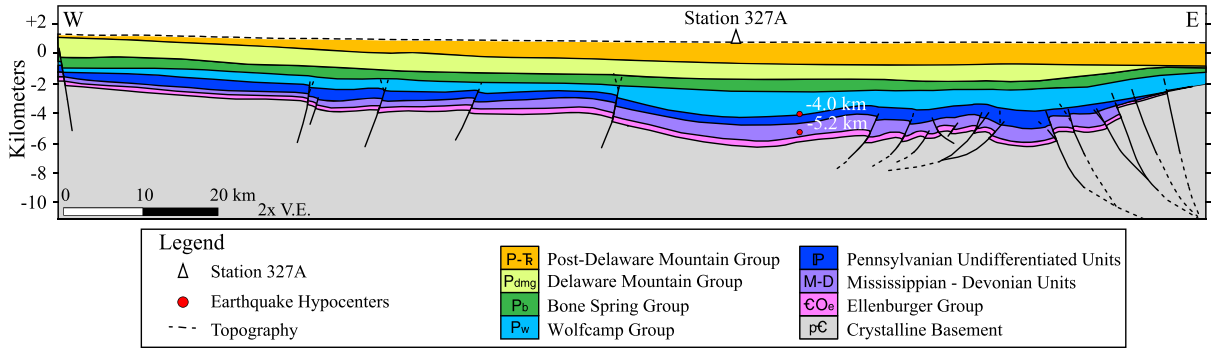

Figure 12. Geological cross section through area of 2009 Pecos Cluster earthquakes (see Figure 1a for location of cross section). Red circles indicate preferred locations. Solid and dashed near-vertical lines indicate imaged faults. This cross section summarizes ongoing analysis of regional stratigraphy and structure by E. Horne and her colleagues at the Texas Bureau of Economic Geology.

The observation that seismicity 2009–2017 extends over a broad geographic area, and is not concentrated around individual high-volume wells, suggests that the high levels of production, associated injection of hydraulic fracturing fluids, and SWD injection influence subsurface pressures regionally, leading to stress changes and earthquakes. This has been observed elsewhere, as in Oklahoma and Kansas (Walsh & Zoback, 2016; Goebel et al., 2018; Peterie et al., 2018; Rubinstein et al., 2018).

4.3. Cultural Implications and Seismic Hazard

The increased levels of seismic activity in the Delaware Basin are a concern as they pose a potential threat to ongoing petroleum development (Figure 2). It is desirable to understand whether this seismic activity is tolerable or whether it poses a hazard that requires modifying regional production practices. Up to the present, the hazard has been minimal, as the largest recorded West Texas earthquake since 2010 occurred on 22 December 2018, and had a magnitude of only M_L3.7. If we extrapolate the straight-line portions of magnitude-frequency plots such as Figure 13, it suggests that activity associated with the Pecos Cluster is unlikely to generate earthquakes with magnitudes larger than about M4.0. However, it is not clear that this extrapolation, even for recent events (e.g., Petersen et al., 2018), is an appropriate approach to evaluate hazard from induced earthquakes, as it does not take account of past or future changes in subsurface conditions caused by human actions, and because our catalog only samples an interval of about 20 years duration. Also, the observation that the *b* value is about 1.5 for earthquakes larger than about M2.5 might indicate that earthquakes with magnitudes as large as M4.0 are unlikely. Of course, because this portion of the magnitude-frequency plot is controlled by the largest few events, the occurrence in the future of several earthquakes with magnitudes of M3.7–M4.0 would make the whole distribution consistent with a *b* value of 1.0.

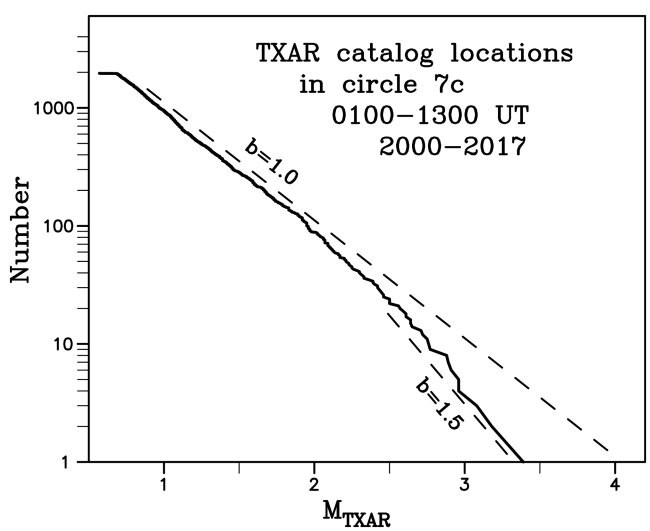

Figure 13. Cumulative number vs magnitude for seismic events within Pecos Cluster (Circle 7c). We plot only events occurring 0100–1300 UTC (nighttime in West Texas) to avoid possible contamination by quarry blasts.

4.4. Ongoing and Future Investigations

A limitation of the present study is that the TXAR catalog epicenters are not accurate enough to support detailed modeling efforts. The epicentral uncertainties are typically about 15–25 km, complicating efforts to associate events with individual wells or known mapped faults. Also, the TXAR catalog provides no information about focal depth, which is essential for associating events with particular strata where injection or production takes place.

One way to address this limitation is to compare TXAR records from 2000 to August 2017 with records collected in September 2017 and subsequently, when TexNet was fully operational and accurate hypocentral locations are available. TexNet locations for many of these post-

September 2017 events were within the Pecos Cluster, and thus, their seismograms at TXAR should be highly similar to some 2000 to August 2017 events. By cross-correlating TXAR records from 2000 to August 2017 earthquakes with TXAR records of post-September 2017 earthquakes having well-determined focal depths, we could obtain more accurate epicenters and credible estimates of focal depth for many of the 2000–2017 events in the TXAR catalog.

Because of the long history of petroleum development in the Delaware Basin, detailed information is available concerning regional crustal structure, the nature of existing faults, reservoir competency and continuity, changing fluid pressures and ambient stress state, and other factors that may impact seismicity. Using the results of the present study and the more accurate TexNet locations from September 2017–2019, we are continuing to investigate how subsurface geology and petroleum development affect the spatiotemporal development of seismic activity. We especially hope this analysis will elucidate why the Pecos Cluster developed after 2009 in Reeves County while there has been only limited seismicity to the north in Ward and Winkler Counties, counties where there has been considerable petroleum production and wastewater disposal since 2000 (see Figures S5–S7).

5. Summary and Conclusions

Since 2015, the USGS has reported numerous earthquakes occurring near the town of Pecos in Reeves County, West Texas. But when this Pecos Cluster first became active has been uncertain because detection and location of small-magnitude earthquakes was problematic in West Texas prior to 2017, when a statewide seismic network (TexNet) was installed. We here illuminate the time history of Pecos Cluster activity by evaluating seismic waveforms crossing the Lajitas TXAR array situated 240 km south of Pecos.

We show that the Pecos Cluster first became active in 2009, when several earthquakes occurred near the town of Pecos. Subsequently, activity rates have increased considerably, with more than 2,000 earthquakes occurring in 2017. Fortuitously, the EarthScope TA was deployed in West Texas in 2009; analysis of seismograms recorded by TA stations indicates that the 2009 events had focal depths of 4.0–5.2 km BSL, within or just below strata where petroleum production and/or fluid waste disposal has been ongoing.

Similarly increasing rates for seismic activity, petroleum production, fluid waste injection, and hydrofracturing activity suggest that petroleum-related activities may be responsible for inducing the seismic activity in the Pecos Cluster between 2009 and 2017. But it is unclear what activity specifically initiated the Pecos Cluster in 2009, or which activity or combination of activities are most responsible for the subsequent increases in seismicity.

Acknowledgments
We thank two anonymous reviewers for suggestions that greatly improved this manuscript. This research was supported by the TexNet program through the University of Texas Bureau of Economic Geology. The authors declare they have no conflicts of interest. Locations determined by TexNet stations are available online; epicenters for West Texas and New Mexico determined from TXAR data are available in Data Set S1 (TXAR catalog) in the supporting information. All seismograms analyzed for this study are available from the IRIS Data Management Center. TexNet seismograms are from the TX network (doi: https://doi.org/10.7914/SN/TX). TXAR data are from the IM network (doi: https://doi.org/10.7914/SN/IM). Seismograms analyzed from 2008 to 2010 were primarily from the TA network (doi:10.7914/SN/TA) and that analysis was supplemented with seismograms from networks 6C (doi:10.7914/SN/6C), EP (doi:10.7914/SN/EP), XR (doi:10.7914/SN/XR), and US (doi:10.7914/SN/US). The petroleum production and wastewater injection data in this investigation are available online from the Texas Railroad Commission (see www.rrc.state.tx.us/oil-gas). We also utilized data concerning hydraulic fracturing provided by FracFocus, a publicly available, online (see www.fracfocus.org), voluntary disclosure database launched by the Ground Water Protection Council.

References

Doser, D. I. (1987). The August 16, 1931, Valentine, Texas, earthquake: Evidence for normal fauting in West Texas. *Bulletin of the Seismological Society of America*, *77*, 2005–2017.

Doser, D. I., Baker, M. R., Luo, M., Marroquin, P., Ballesteroros, L., Kingwell, J., et al. (1992). The not so simple relationship between seismicity and oil production in the Permian Basin. *West Texas, Pure Appl. Geophysics*, *139*, 481–506.

Ellsworth, W. L. (2013). Injection-induced earthquakes. *Science*, *341*, 1225924. https://doi.org/10.1126/science.1225942

Frohlich, C. (2012). Two-year survey comparing earthquake activity and injection well locations in the Barnett Shale, Texas. *Proceedings of the National Academy of Sciences*, *109*(35), 13,934–13,938. https://doi.org/10.1073/pnas.1207728109

Frohlich, C., & Davis, S. D. (2002). *Texas earthquakes* (p. 275). Austin, TX: University of Texas Press.

Frohlich, C., DeShon, H. R., Stump, B., Hayward, C., Hornbach, M. J., & Walter, J. I. (2016). A historical review of induced earthquakes in Texas. *Seismological Research Letters*, *87*(4), 1022–1038. https://doi.org/10.1785/0220160016

Frohlich, C., Ellsworth, W. L., Brown, W. A., Brunt, M., Luetgert, J. H., MacDonald, T., & Walter, S. (2014). The 17 May 2012 M4.8 earthquake near Timpson, east Texas: An event possibly triggered by fluid injection. *Journal of Geophysical Research: Solid Earth*, *119*, 581–593. https://doi.org/10.1002/2013JB010755

Goebel, T. H. W., Weingarten, M., Chen, X., Haffener, J., & Brodsky, E. E. (2017). The 2016 Mw5.1 Fairview, Oklahoma earthquakes: Evidence for long-range poroelastic triggering at >40 km from fluid disposal wells. *Earth and Planetary Science Letters*, *472*, 50–61. https://doi.org/10.1016/j.epsl.2017.05.011

Hornbach, M. J., DeShon, H. R., Ellsworth, W. L., Stump, B. W., Hayward, C., Frohlich, C., et al. (2015). Causal factors for seismicity near Azle, Texas. *Nature Communications*, *6*, 6728. https://doi.org/10.1038/ncomms7728

Keller, G. R., Rogers, A. M., & Orr, C. D. (1987). Seismic activity in the Permian Basin of West Texas and southeastern New Mexico. *Seismological Research Letters*, *58*, 63–70.

Lund-Snee, J.-E., & Zoback, M. D. (2016). State of stress in Texas: Implications for induced seismicity. *Geophysical Research Letters*, *43*, 10,208–10,214. https://doi.org/10.1002/2016GL070974

Lund-Snee, J.-E. & Zoback, M. D. (2018). State of stress in the Permian Basin, and Texas and New Mexico: Implications for induced seismicity. *The Leading Edge 37*(2), 127-134. https://doi.org/10.1190.tle37020127.1

OGJ editors (2018). IHS Markit forecasts Permian basin oil production will double from 2018-23. *Oil & Gas Journal*, *116*. https://www.ogj.com/articles/2018/06/ihs-markit-forecasts-permian-basin-oil-production-will-double-from-2018-23.html

Peterie, S. L., Miller, R. D., Intfen, J. W., & Gonzales, J. B. (2018). Earthquakes in Kansas induced by extremely far-field pressure diffusion. *Geophysical Research Letters*, *45*, 1395–1401. https://doi.org/10.1002/2017GL076334

Petersen, M. D., Mueller, C. S., Moschetti, M. P., Hoover, S. M., Rukstales, K. S., McNamara, D. E., et al. (2018). One-year seismic hazard forecast for the central and eastern United States from induced and natural earthquakes. *Seismological Research Letters*, *89*, 1049–1061. https://doi-org.ezproxy.lib.utexas.edu/10.1785/0220180005

Rubinstein, J. L., Ellsworth, W. L., & Dougherty, S. L. (2018). The 2013-2016 induced earthquakes in Harper and Sumner counties, southern Kansas. *Bulletin of the Seismological Society of America*, *108*(2), 674–689. https://doi.org/10.1785/0120170209

Savvaidis, A., Young, B., Huang, G.-C. D., & Lomax, A. (2019). TexNet: a statewide seismological network in Texas. *Seismological Research Letters*, *90*, 1702–1715. https://doi-org.ezproxy.lib.utexas.edu/10.1785/0220180350

Scales, M. M., DeShon, H. R., Magnani, M. B., Walter, J. I., Quinones, L., Pratt, T. L., & Hornbach, M. J. (2017). A decade of induced slip on the causative fault of the 2015 MW4.0 Venus earthquake, northeast Johnson County, Texas. *Journal of Geophysical: Research*, *122*, 7879–7894. https://doi.org/10.1002/2017JB014460

Scanlon, B. R., Reedy, R. C., Male, F., & Walsh, M. (2017). Water issues related to transitioning from conventional to unconventional oil production in the Permian Basin. *Environmental Science & Technology*, *51*, 10,903-10,912. https://doi.org/10.102/aces.est.7b02185

Skoumal, R. J., Riles, R., Brudzinski, M. R., Barbour, A. J., & Currie, B. S. (2018). Earthquakes induced by hydraulic fracturing are pervasive in Oklahoma. *Journal of Geophysical Research: Solid Earth*, *123*, 10,918-10,935. https://doi.org/1029/1018JB016790

Tibuleac, I., & Herrin, E. (1997). Calibration studies at TXAR. *Seismological Research Letters*, *68*(2), 353–365.

Waldhauser, F., & Ellsworth, W. L. (2000). A double-difference earthquake location algorithm: Method and application to the northern Hayward fault, California. *Bulletin of the Seismological Society of America*, *90*, 1353–1368.

Walsh, R. R., & Zoback, M. D. (2016). Probabilistic assessment of potential fault slip related to injection-induced earthquakes: Application to north-central Oklahoma. *USA, Geology*, *44*, 991–994. https://doi.org/10.1130/G38275.1

Walter, J. I., Frohlich, C., & Borgfeldt, T. (2018). Natural and induced seismicity in the Texas and Oklahoma Panhandles. *Seismological Research Letters*, *89*(6), 2437–2446. https://doi.org/10.1785/0220180105

Erratum

Due to a typesetting error, an outdated version of the Supporting Information was originally published. The revised version of Data set S1 replaced incorrect values in column F [distTXAR] for the source-to-station distance by calculating them directly from the analyst-read S – P times [column K] using eq. (1) in the text. The authors then applied the corrected values for distTXAR to recalculate the latitude and longitude [xlatTXAR and xlonTXAR in columns B and C]. The original and corrected locations were nearly the same, so these changes did not affect the results and conclusions of the study. The originally published version of the Supporting Information has been replaced, and this may be considered the official version of record.